IL NUOVO CIMENTO Vol. 34 C, N. 2 Marzo-Aprile 2011
DOI 10.1393/ncc/i2011-10842-9

Colloquia: WISH2010

Recent results from the Pierre Auger Observatory

A. Insolia for the Pierre Auger Collaboration(*)
Dipartimento di Fisica e Astronomia, Università di Catania - Catania, Italy

(ricevuto il 23 Novembre 2010; approvato il 20 Dicembre 2010; pubblicato online il 30 Marzo 2011)

Summary. — Since June 2008 the Pierre Auger Observatory has been taking data in its final configuration. Since then two main upgrades have been completed: the High Elevation Angle Telescopes (HEAT) and an infill in the surface region covered by HEAT, with the main goal of bringing the energy threshold down to 10^{17} eV. In this paper, I will give an overview of the main recent results of the Auger Observatory. More specifically, I will discuss the all-particle energy spectrum and the evidence for the GZK features, the measurement of the elongation rate and the evidence for anisotropy in the subset of the highest energy events. Systematic uncertainties will be discussed.

PACS 96.50.sd – Extensive air showers.
PACS 98.70.Sa – Cosmic rays (including sources, origin, acceleration, and interactions).

1. – Introduction

The Pierre Auger Observatory is designed to measure high-energy cosmic rays above 10^{18} eV with unprecedented statistics and precision. The Southern Observatory, close to the city of Malargüe in Argentina, was completed in June 2008 and has recorded data in a stable manner since 2004 while the deployment went on. It is equipped with two independent detectors of cosmic rays. The Surface Detector (SD) is a grid of more than 1600 equally spaced Cherenkov water tanks, extending over an area of 3000 km^2, sampling the lateral density of shower particles at ground level. The Fluorescence Detector (FD) is made up of 4 fluorescence sites, equipped with 6 telescopes each, overlooking the atmosphere above the array to observe the fluorescence light emitted by the nitrogen molecules as the shower particles traverse the atmosphere. The hybrid design of the Observatory has enormous advantages for cosmic-ray studies. It offers actually the

(*) Observatorio Pierre Auger - Av. San Martin Norte 304, 5613 Malargue, Argentina. (Full author list: http://www.auger.org/archive/authors_2010_08.html.)

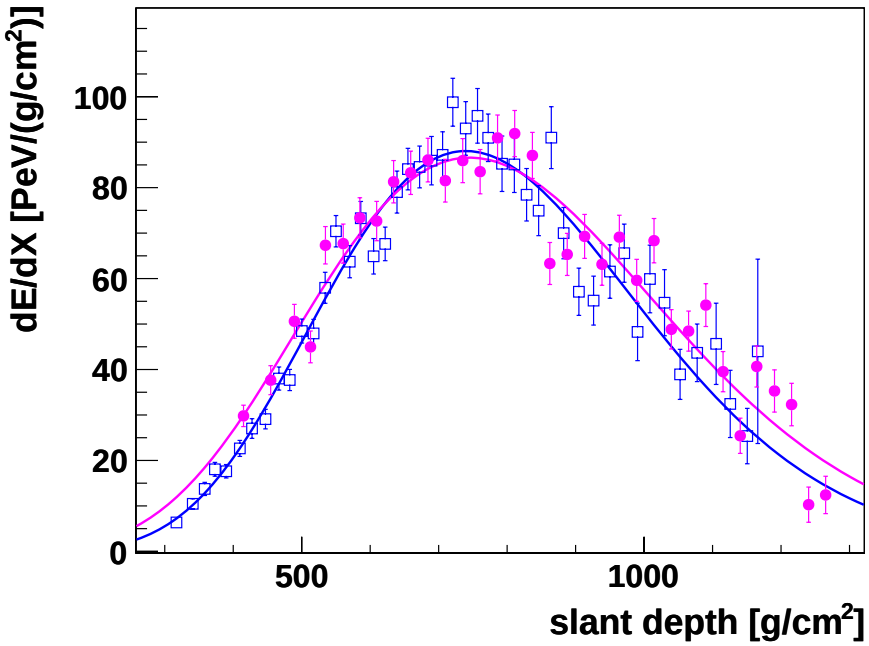

Fig. 1. – (Color online) A sample longitudinal profile measured at the Observatory, as reconstructed independently by two fluorescence detectors: Coihueco (open blue squares, $E = 56 \pm 4\,\mathrm{EeV}$, $X_{max} = 740 \pm 10\,\mathrm{g/cm^2}$) and Los Morados (magenta filled dots, $E = 62 \pm 5\,\mathrm{EeV}$, $X_{max} = 745 \pm 14\,\mathrm{g/cm^2}$).

possibility of performing independent measurements of the same event. The FD provides a calorimetric determination of the primary energy and of the Shower Detector Plane (SDP). The FD takes data only in clear moonless nights with a duty cycle of the order of 14%. The SD, on the other side takes data 24 hour a day and produces a large statistical sample. A very important feature of the hybrid design of the Observatory is that the SD can be actually calibrated using the so-called hybrid events: events that can be fully reconstructed by both detectors. This procedure avoids comparison with Monte Carlo (MC) simulations for the energy calibration. In this paper we will present, in the first place, a short overview of the calibration procedure. We will then discuss the energy spectrum, composition studies in more detail and some aspects of the small-scale anisotropy analysis.

2. – All-particle energy spectrum

The FD provides a measurement of the so-called longitudinal profile, that is its recorded light profile at the telescopes, as a combination of direct and scattered light components. These components are first deconvoluted in all different contributions and then converted into energy deposit at a given atmospheric depth along the shower axis, using the light attenuation factors measured at the Observatory by atmospheric monitoring devices [1], and the fluorescence and Cherenkov yields from [2] and [3]. The method currently adopted to reconstruct the energy deposit profiles is presented and detailed in [4]. In fig. 1 the energy deposit profile of a hybrid event measured at the Observa-

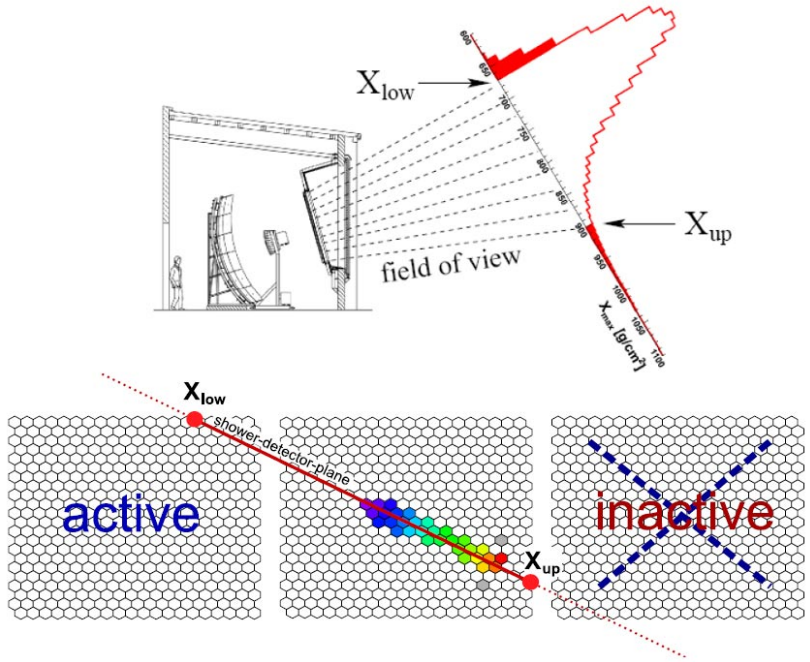

Fig. 2. – Illustration of the geometric field of view of the FD telescopes.

tory is shown, as reconstructed independently by two fluorescence detectors. Due to the limited field of view of the telescopes, see fig. 2, only part of the development is observed, therefore for the extrapolation to unobserved depths, a fit of the measured profiles is performed using a Gaisser-Hillas function [5]. The integral of the fitted function returns the calorimetric energy of the shower, and the depth at which the maximum occurs is X_{max}. The accuracy with which the depth of maximum is reconstructed from hybrid data has been studied in detail by comparing the reconstructed and generated X_{max} from detailed MC simulations. A small energy-dependent reconstruction bias is present, especially at low energies: on average it is estimated to be smaller than $5\,\mathrm{g/cm^2}$ for protons and smaller than $2\,\mathrm{g/cm^2}$ for iron nuclei. This estimate includes possible biases due to the hybrid geometry reconstruction, Cherenkov and fluorescence light contributions and parameters of the longitudinal energy deposit profile. Actually, other sources of systematics have been studied, like the impact of different profile fitting functions, alternative algorithms for the reconstruction of the energy deposit profiles, and the systematics related to the description of the lateral Cherenkov and fluorescence light distributions in the shower.

Overall, we report a systematic uncertainty in the X_{max} reconstruction equal to $+8/-6\,\mathrm{g/cm^2}$ at one EeV. The sampling of the shower front at the detection level obtained with the SD provides a measurement of the Lateral Distribution Function (LDF). The LDF fit allows to extract the signal intensity at 1000 m from the shower axis, $S(1000)$, which can be considered a good estimator for the cosmic-ray energy [6]. Due to the attenuation in the atmosphere, $S(1000)$ depends on the zenith angle (we expect a larger signal for a vertical shower than for an inclined one if both are induced by primaries of the same energy). The Constant Intensity Method (CIC) [7] is used to rescale the signal intensity

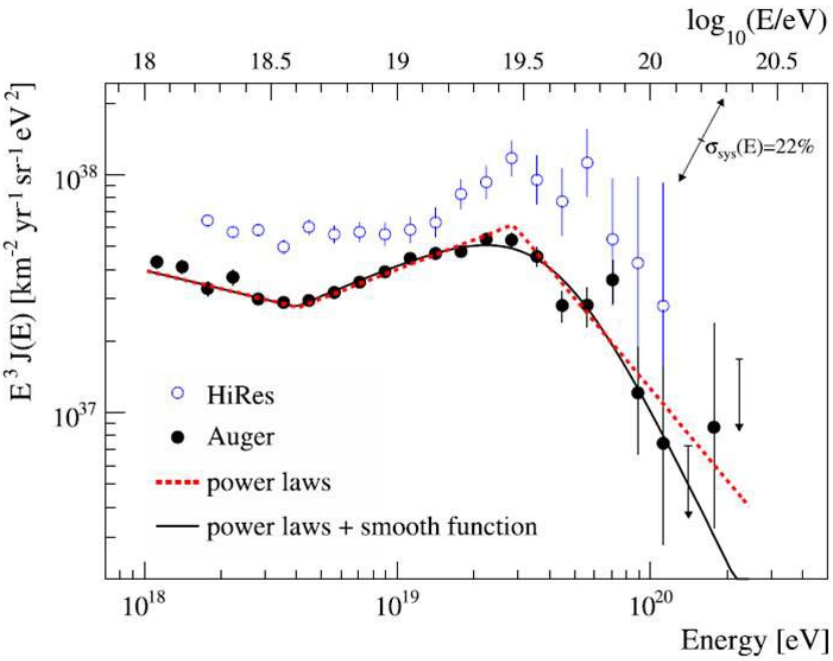

Fig. 3. – The all-particle spectrum measured by the P. Auger Collaboration in comparison with the HiRes data. The systematic uncertainty of the flux scaled by E^3 due to the uncertainty of the energy scale is 22%.

to the median of the zenith angle distribution ($\theta = 38^\circ$ if we consider angles $\leq 60^\circ$). The CIC method [7] provides the new SD energy estimator $S_{38^\circ}(1000)$. For a sample of hybrid events the correlation between $S_{38^\circ}(1000)$ and the corresponding primary energy, obtained with the FD calorimetric measurement, produces the empirical relation which allows to transfer the energy calibration to all SD events. Additional details can be found in ref. [6]. The energy spectrum is shown in fig. 3. The measured all-particle spectrum shows a suppression of the flux above about 5×10^{19} eV. The spectrum can be described by a broken power law $E^{-\gamma}$ with $\gamma = 3.26 \pm 0.04$ below the ankle which is measured at $\log_{10}(E_{ankle}/\mathrm{eV}) = 10^{18.6}$. Above the ankle the spectrum is described by a power law with spectral index $\gamma = 2.59 \pm 0.02$ followed by a flux suppression. The significance of the suppression is larger than 20σ. The suppression is similar to what is expected for the GZK effect for protons or nuclei. It could also be related to a change of the shape of the average injection spectrum at the sources. The question is still open and debated.

3. – Composition reconstruction with the Fluorescence Detector

We will devote more room for the composition studies. The main reason is that the measurement of mass composition is crucial for cosmic-ray understanding above 10^{17} eV. For instance, it represents a key observable for the explanation of the features observed in the energy spectrum, such as the nature of the "ankle" observed around $10^{18.6}$ eV and of the flux suppression observed above 5×10^{19} eV [6,8]. Moreover it becomes of relevant importance also for what concerns anysotropy studies: for instance, a consistent correlation analysis with astrophysical objects requires the knowledge of the primary mass.

The composition feature at the basis of FD analysis is the different longitudinal development exhibited by primaries of different masses. Showers induced by heavy nuclei develop faster in the atmosphere with respect to light nuclei because of the higher cross section with air, *e.g.* on average they are expected to exhibit the depth of maximum X_{max} at smaller atmospheric depths. Furthermore, showers of the same primary energy and mass do not have the same development in the atmosphere. Such shower-to-shower fluctuations originate from fluctuations in the first interaction point high in the atmosphere and from the statistical nature of the interactions as the cascade develops. Such shower-to-shower fluctuations are smaller for heavy primaries compared to light nuclei, as they are averaged over more nucleonic sub-showers, if one follows the simple approximation of the superposition model. It is thus possible to use the average X_{max} and its fluctuations as a function of the primary energy to extract the composition information.

The use of the spread of the X_{max} distribution around its average value as a function of the primary energy for the investigation of the mass composition is discussed in the next section for hybrid data.

For composition studies performed with the FD, only hybrid events are considered, *e.g.* showers triggering the fluorescence telescopes and some ground stations in coincidence, providing additional timings needed to achieve a more precise reconstruction of the shower axis ($< 0.6^\circ$). The additional timing information of the surface stations is crucial to constrain the geometry fit and achieve a better resolution of the shower axis. This will be a huge benefit for composition studies, as the reconstruction precision of the longitudinal profile is related to that of the shower geometry.

3˙1. *Hybrid event selection.* – The composition analysis presented here is based on a set of hybrid data recorded at the Observatory in the period from December 2004 to March 2009 [9]. A severe selection has to be applied to the event sample to guarantee a precise and unbiased measurement of the average X_{max} and its fluctuations. The applied list of quality cuts can be classified in four general categories: calibration, atmosphere, geometry and profile selection.

Calibration selection: The response of the FD camera is monitored each night of data taking. Calibration data has been analyzed for the above-cited period and pixels with anomalous behavior have been identified and classified as "bad". The presence of such pixels in the event typically causes sudden drops in the reconstructed profiles. Events of this kind are therefore rejected.

Atmosphere selection: A large concentration of clouds in the field of view or poor aerosol conditions can significantly distort the observed longitudinal profiles. The amount of clouds and the aerosol profiles can be measured by the Lidar stations at each FD site and by the Central Laser Facility (CLF) at the center of the array. Events recorded with a cloud coverage larger than 25% and with a vertical aerosol optical depth (VAOD) at 3 km larger than 0.1 are rejected.

Geometry selection: Since the trigger probability of the surface stations depends on the mass of the primary particle [10], increasing with energy and decreasing with zenith angle θ and shower plane distance d_{tank} to the core, the hybrid requirement might introduce a bias in the measurement of the average X_{max}, especially at low energies. Therefore, an energy-dependent fiducial cut on θ and d_{tank} is applied to keep the trigger probability close to unity.

Profile selection: A successful Gaisser-Hillas fit to the experimental profiles is required: the reduced χ^2 has to be smaller than 2.5 and to reject unreliable X_{max} it is required that the χ^2 of a linear fit to the profile exceeds the Gaisser-Hillas fit χ^2 by at least four.

Only showers reconstructed with good precision are selected: the estimated uncertainties in the reconstructed X_{max} and total energy must be smaller than $40\,\mathrm{g/cm^2}$ and 20%, respectively.

Furthermore, the X_{max} has to be observed in the geometrical telescope field of view, as shown in fig. 2, delimited by the smaller and the higher observed depth X_{low} and X_{up}. This cut has the effect of rejecting very deep or very shallow showers and causes a bias in the event selection towards light primaries, which are more preferred in the selection.

To avoid such bias, we followed the strategy of requiring the X_{max} to be inside a fiducial range (the viewable FOV), which varies from event to event, instead of inside the fixed geometrical FOV. The viewable FOV depends on the shower geometry (geometrical FOV, telescope-shower distance), but also on the shower energy and atmospheric conditions. The fiducial range is directly determined from data, without introducing uncertainties related to MC simulations. It can be demonstrated that this procedure allows a determination of the $\langle X_{max}\rangle$ and RMS with a bias less than 3 and $5\,\mathrm{g/cm^2}$, respectively.

The full chain of quality cuts have been applied to about 1.4×10^6 raw hybrid events. 3754 events have been selected for physics analysis.

The total X_{max} resolution (detector+atmosphere), given the described set of quality cuts, has been determined from detailed MC simulations and cross-checked with stereo data at the highest energies. It deteriorates at low energies, around $27\,\mathrm{g/cm^2}$ at 1 EeV, and improves to $20\,\mathrm{g/cm^2}$ at 10 EeV. We note that such values are smaller than the average separation between proton and iron primaries ($\sim 100\,\mathrm{g/cm^2}$).

The systematic uncertainties affecting the measurement of $\langle X_{max}\rangle$ and RMS have been also carefully studied in their contributions, mainly uncertainties related to the atmospheric properties, calibration conditions, event reconstruction and mass acceptance. These add up to a total estimated systematic uncertainty of $\langle X_{max}\rangle$ that is $< 13\,\mathrm{g/cm^2}$ and $< 6\,\mathrm{g/cm^2}$ for the RMS.

3˙2. *Mass composition results.* – We report in fig. 4 the average depth of maximum as a function of the primary energy (black filled dots) measured from hybrid data after applying the described list of quality cuts. The change of $\langle X_{max}\rangle$ per decade of energy is called "elongation rate" and is sensitive to changes of composition with energy. The prediction for $\langle X_{max}\rangle$ *vs.* energy for different high-energy hadronic models (QGSJET01, QGSJETII, SIBYLL 2.1, EPOS 1.99) are reported for protons (upper lines in fig. 4) and for iron (lower lines in fig. 4). It has to be noted that a simple line fit does not describe our data very well ($\chi^2/\mathrm{Ndf} = 34.9/11$), while allowing for a break energy leads to a satisfactory fit ($\chi^2/\mathrm{Ndf} = 9.7/9$). As can be seen, the measurement shows evidence for an increasing average nuclear mass as a function of the energy in the elongation rate and its fluctuations. The results were found to be independent of zenith angle, time periods and FD stations within the quoted uncertainties.

A change of the elongation rate slope is clearly observed around $10^{18.24}\,\mathrm{eV}$, pointing towards a change of composition with energy around the ankle and supporting the hypothesis of a transition from galactic to extragalactic cosmic rays in this region. The current uncertainties in the hadronic interaction models do not lead to an unambiguous interpretation of the absolute elongation rate values especially at the highest energies. However, if these models provide a realistic description of hadronic interactions at high energies, the comparison of the data and simulations leads to the conclusion that a gradual increase of the average mass of cosmic rays with energy up to 59 EeV is observed.

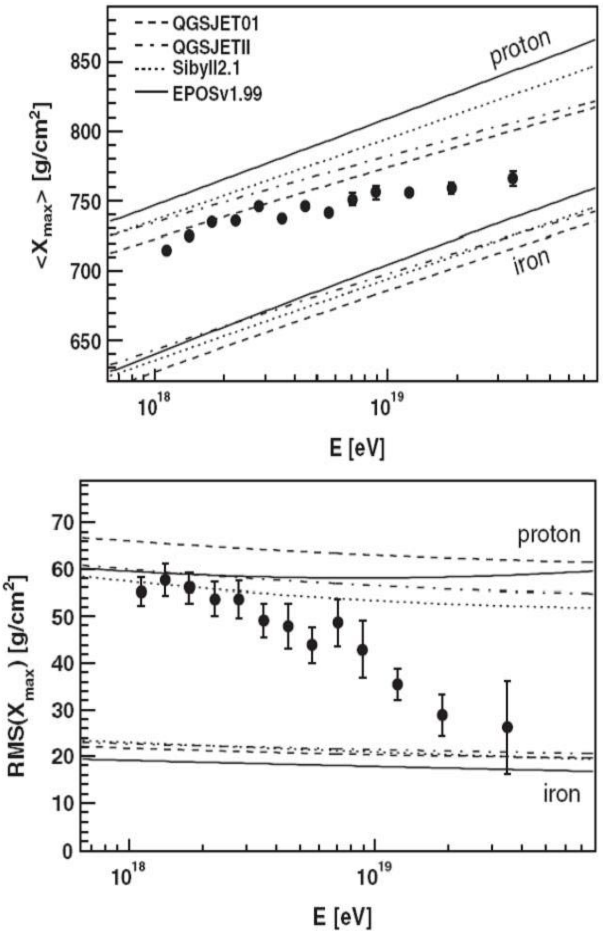

Fig. 4. – Average X_{max} and RMS(X_{max}) as a function of energy.

In fig. 5 we report in filled black dots the measured RMS(X_{max}) as a function of the primary energy, as compared with hadronic model predictions. This has been calculated by subtracting in quadrature the detector resolution from the width of the observed X_{max}. The fluctuations are observed to decrease with energy. Such result, given the same considerations made above, constitutes an independent confirmation of the increase of primary mass with energy [9].

4. – Composition reconstruction with the Surface Detector

Large efforts have been carried out recently within the Collaboration to investigate the possibility of reconstructing the composition information from Surface Detector data [11]. This is particularly important as the SD is providing a larger event statistics than the hybrid ones, the sources of systematic uncertainties are different and an independent cross-check of the composition results presented for the FD can be made.

The best observable for composition studies based on SD data is the number of muons/electrons, which is not directly accessible in Surface Detector tanks. Nevertheless,

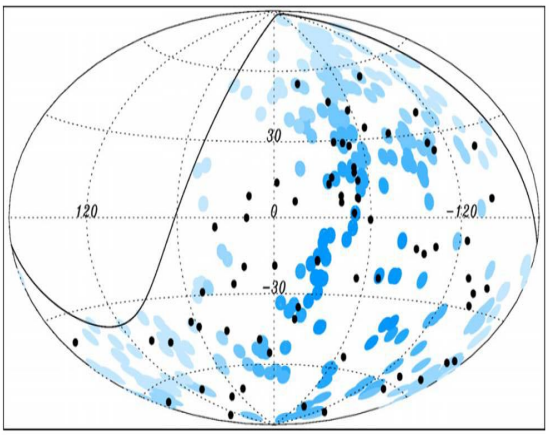

Fig. 5. – The 69 arrival directions of CRs with energy larger than 55 EeV detected by the P. Auger Observatory up to 31 December 2009 (black dots) in an Aitoff-Hammer projection of the sky in galactic coordinates. The positions of 318 AGN (within 75 Mpc) in the VCV catalog are reported as circles of radius 3.1°. The solid line represents the field of view of the Southern Observatory for zenith angles smaller than 60°. The exposure-weighted fraction of the sky covered by the AGN circles is 21%.

some "indirect" observables, related to the shower development and the amount of muons, have been investigated to reconstruct composition from SD data. These variables are the signal rise time (the time it takes for the recorded FADC signal to go from 10% to 50% of the total signal) and its asymmetry observed in ground stations. This work is in progress and is not going to be discussed in the present paper. Preliminary results as well as additional details can be found in ref. [12]. I will simply mention that preliminary results obtained with SD data are in agreement with the FD elongation rate.

5. – Small-scale anisotropy

The search for the origin of the highest cosmic rays has been a great challenge since the beginning of the cosmic-ray adventure long ago. On the other end, giant arrays, like the P. Auger Observatory, will allow, on a time scale of the order of 10 years, the possibility to detect a large sample of events at the highest energies. This will open a new window on the Universe: the charged particle astronomy. It will be possible to search for cosmic-ray sources since the deviation from a straight-line path due to the intergalactic and galactic magnetic fields is quite small, above 10^{19} eV for path lengths of the order of the GZK radius (100–200 Mpc). In addition, within the GZK radius the luminous matter distribution of the Universe is not isotropic. Therefore one can argue about the possibility to point given astrophysical sources or to detect anisotropy in the arrival distributions of the highest energy cosmic rays. The CRs detected at the P. Auger Observatory with energies larger than the expected GZK cutoff energy are of the greatest interest under this aspect. The P. Auger Collaboration has investigated this specific point and published correlation studies with the Véron-Cetty and Véron (VCV) catalog [13] as well as with other catalogs: 2MASS Redshift Surveys (2MRS) [14] and Swift Burst Alert Telescope (Swift-BAT) [15] catalogs.

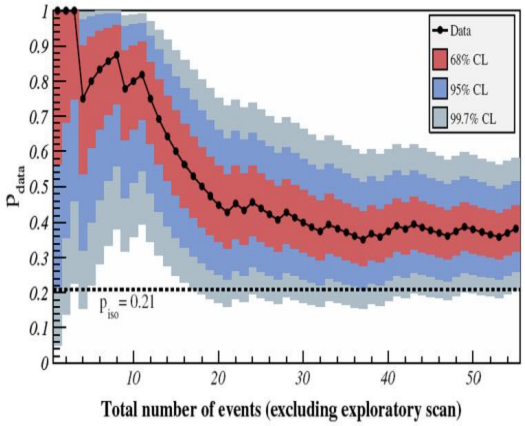

Fig. 6. – The most likely value of the degree of correlation $p_{data} = k/N$ (black dots) plotted as a function of the time-ordered events excluding the events of the initial exploratory scan. The 68%, 95% and 99.7% regions around the dots are shown. The horizontal dashed line shows the p-value for the expectation of isotropy.

I will briefly summarize the status of the search while for a detailed discussion one should refer to the papers quoted in ref. [16].

Using data collected through 31 August 2007, The P. Auger Collaboration has reported a correlation with the arrival direction of ultra high energy cosmic rays with energies larger than or equal to 55 EeV and the positions of the nearby objects from the VCV catalog of quasars and active galactic nuclei (AGN). The null hypothesis of isotropy was rejected with 99% confidence level based on a single-trial test motivated by early data and confirmed by the data collected subsequently to the definition of the test. An update of this analysis has been recently published including events detected up to 31 December 2009. This event sample (with exactly the same reconstruction algorithm, energy calibration and quality cuts for event selection as in the exploratory scan) consists of 69 arrival directions. The same conditions for the comparison were applied: the angular distance from the AGNs is still 3.1°, as in the exploratory scan. Only AGNs in the VC catalog with redshift $z \leq 0.018$ were considered. The arrival direction of the 69 CRs are reported in fig. 5 and compared with the positions in galactic coordinates of 318 AGNs from the VCV catalog [16]. The exposure-weighted fraction of the sky covered by the 3.1° angular regions around the AGNs is 21%. In other words, this is the fraction of events that one expects to correlate under the hypothesis of isotropy.

The current status is better seen in fig. 6 where the degree of correlation $p_{data} = k/N$ (black dots) is plotted as a function of the time-ordered events excluding the events of the initial exploratory scan. The 68%, 95% and 99.7% regions around the dots are also shown. The horizontal dashed line shows the p-value for the expectation of isotropy. The current estimation for the correlation fraction is 38% (as can be easily seen from fig. 6). A 5σ significance will require 165 events excluding the exploratory scan. With the expected arrival frequency in this energy region we can foresee that such a larger data set will not be available for at least another four years. That is why it is quite natural, in the meantime, to explore the present data set to see if scenarios other than the simple VCV correlation are supported by the current set of arrival directions. We have therefore

examined cross-correlation analysis between arrival directions of CRs and positions of the objects in the 2MRS [14] and Swift-BAT [15] catalogs. Only astrophysical objects within 200 Mpc were considered and in the case of the 2MRS catalog a region ($\pm 10^\circ$) around the galactic plane was excluded, due to incompleteness of the 2MRS catalog in the galactic plane region.

We have observed correlations in excess of expectations based on the hypothesis of isotropy in all the considered cases. The current results are quite interesting but definitive conclusions must wait for additional data. For a detailed discussion of these points one can see ref. [16].

6. – Conclusions

In this paper we have presented a short discussion of the recent results from the Pierre Auger Observatory on the all-particle energy spectrum, composition results and anisotropy studies. We have presented the experimental evidences for the flux suppression above about $\log_{10}(E/\mathrm{eV}) = 19.5$ in the energy spectrum. The flux suppression is confirmed with a very high significance level (20σ). We have got indication for a mixed composition and an increasing average nuclear mass as a function of the energy in the elongation rate and its fluctuations. The interpretation of the experimental findings for the elongation rate is very challenging and demanding. Additional work will be required. Quite soon the analysis performed with hybrid data will be extended in the low-energy regime (10^{17}–10^{18} eV) with the detector enhancements (High Elevation Angle Telescopes) recently installed at the Observatory [17], crucial to study the transition from galactic to extragalactic cosmic rays. Finally, we have evidence for anisotropy in the arrival direction of the highest energy cosmic rays (energy larger than or equal to 55 EeV). Anyway, for definitive conclusions as well as for the possibility to disentangle contributions from individual sources we must wait for additional data.

REFERENCES

[1] Abraham J. *et al.* (P. Auger Collaboration), *Astropart. Phys.*, **33** (2010) 108.
[2] Ave M. *et al.* (AIRFLY Collaboration), *Astropart. Phys.*, **28** (2007) 41; Nagano M. *et al.*, *Astropart. Phys.*, **22** (2004) 235.
[3] Nerling F. *et al.*, *Astropart. Phys.*, **24** (2006) 421.
[4] Unger M. *et al.*, *Nucl. Instrum. Methods A*, **588** (2008) 433.
[5] Gaisser T. K. and Hillas A. M., *Proc. 15th ICRC*, **8** (1977) 353.
[6] Abraham J. *et al.* (P. Auger Collaboration), *Phys. Rev. Lett.*, **101** (2008) 061101; *Phys. Lett. B*, **685** (2010) 239.
[7] Hersil J. *et al.*, *Phys. Rev. Lett.*, **6** (1961) 22.
[8] Abbasi R. U. *et al.* (HiRes Collaboration), *Astropart. Phys.*, **32** (2009) 53.
[9] Abraham J. *et al.* (P. Auger Collaboration), *Phys. Rev. Lett.*, **104** (2010) 091101.
[10] Allard D. (P. Auger Collaboration), *Proc. 29th ICRC* (2005).
[11] Wahlberg H. (P. Auger Collaboration), *Proc. 31st ICRC* (2009).
[12] Riggi S. (P. Auger Collaboration), *CRIS 2010 Proc. Conf., Nucl. Phys. B*, in press.
[13] Véron-Cetty M. P. and Véron P., *Astron. Astrophys.*, **455** (2006) 773.
[14] Jarrett T. H. *et al.*, *Astron. J.*, **119** (2000) 2498.
[15] Tueller J. *et al.*, *Astrophys. J. Suppl.*, **186** (2010) 378.
[16] Abraham J. *et al.* (P. Auger Collaboration), *Science*, **318** (2007) 938; *Astropart. Phys.*, **29** (2008) 188.
[17] Klages H. (P. Auger Collaboration), *in CRIS 2010 Proc. Conf., Nucl. Phys. B*, in press.